

Photonic Signal Generation for Millimeter-Wave Communications

Jeffrey A. Nanzer, Patrick T. Callahan, Michael L. Dennis,
and Thomas R. Clark Jr.

Future wireless communications systems will require data rates on the order of 10 Gb/s and greater to support the increased desire for high-speed data transfer for applications such as wireless personal area networking. Millimeter-wave photonic systems represent a well-suited approach to such broadband wireless communications because of the large bandwidths that can be supported, the favorable propagation characteristics of millimeter-wave radiation, and the ability to remote broadband signals over long distances in optical fiber. This article outlines recent work on millimeter-wave photonic communications systems operating at 40 and 60 GHz, where data rates up to 3 Gb/s are demonstrated. Current research is being conducted on the development of an 80-GHz system with the goal of achieving 10 Gb/s over distances of 100 m.

INTRODUCTION

The millimeter-wave (MMW) region of the electromagnetic spectrum refers to wavelengths on the order of 1–10 mm, or the frequency range of 30–300 GHz. MMW technologies have long been used for military applications, such as radar and missile guidance,¹ as well as scientific purposes, such as radio astronomy and spectroscopy.² The MMW region has been receiving increased attention in recent years in part because of the greater availability, improved performance, and lower cost of components operating at MMW frequen-

cies, leading to new developments and techniques for transmitter and receiver subsystems. Additionally, the Federal Communications Commission has recently allocated various MMW bands up to 100 GHz for commercial use.³ In recent years, there has been a significant increase in MMW applications such as security sensing, medical imaging, and communications. In security sensing, the wavelength of the radiation is small enough to provide high-resolution imaging for the detection of contraband and explosives. Additionally, the propaga-

tion loss through clothing materials is very low (on the order of 1–2 dB at 250 GHz), allowing the detection of concealed contraband.⁴

The focus of this article is MMW communications using photonic signal generation, where the primary benefit is the extremely wide bandwidth supported by optical fiber, which can enable very high data rates relative to current technology, as compared with coaxial cables or waveguides. Current wireless systems generally operate at lower frequencies where components tend to be less expensive; for example, WiFi (IEEE 802.11)-compliant networks operate in the 2.4- to 2.5-GHz band, whereas Global System for Mobile Communications (GSM) cellular telephone systems operate below 2.0 GHz. However, at these frequencies, the bandwidth—and thus the supported data rate—is constrained compared with MMW frequencies. Future wireless networking applications are expected to require much greater bandwidth than is currently available at these low carrier frequencies. IEEE recently defined a high-bandwidth “wireless personal area network” (WPAN) standard, IEEE802.15.3c,⁵ specifying wireless data rates up to 5.28 Gb/s, operating on RF carrier frequencies of 58.3–64.8 GHz. In this article, we describe photonic technologies developed at APL for use in 60-GHz WPAN and point-to-point communication systems. The 60-GHz carrier signal is generated using a dual-wavelength stimulated Brillouin scattering (SBS) laser, and the baseband data are photonicly upconverted to 60 GHz through photomixing. The MMW signal is transmitted through free space using a MMW transmitter and receiver.

One of the challenges of implementing communications systems in the MMW band is the generation of good-quality carrier signals. Common electrical oscillators typically generate stable continuous-wave tones with low phase noise at frequencies in the megahertz range. Microwave signals can be generated from such low-frequency oscillators by frequency multiplication; however, the phase noise of the output frequency is increased by 6 dB with every doubling in frequency, so low-phase-noise MMW carriers are difficult to achieve in this way. This implementation is also complicated and can be costly. MMW oscillators such as impact ionization avalanche transit-time (IMPATT) diode oscillators can generate high-power tones at frequencies greater than 300 GHz; however, because of the avalanche breakdown process required for signal generation the phase noise is very poor. Transferred electron oscillators, such as Gunn diode oscillators (named after John Battiscombe Gunn), can generate frequencies in excess of 100 GHz, and although they display better phase noise than IMPATT diode oscillators, their noise performance is not as good as the potential noise performance of photonicly generated signals. In addition to

the phase noise benefits of photonic signal generation, it is often desirable to feed the carrier signal to multiple remote locations—particularly for communications applications, where the antenna may be well removed from the user—but coaxial cable losses in the MMW region can easily exceed a few decibels per meter for cables of reasonable quality, severely limiting the remoting capabilities of coaxial cables.

In recent years, photonic techniques have emerged that provide promising solutions to the problems encountered in MMW electronic signal generation. Single-sideband encoding of dual-wavelength lasers and photomixing allow for direct upconversion of baseband data onto the MMW carrier signal without the need for local oscillators or frequency multiplication. The wavelength separation defines the MMW carrier and can be set within the bandwidth of the optical components, which can theoretically support frequencies in the hundreds of gigahertz. Additionally, the phase noise of the photonicly generated MMW carrier is independent of frequency and depends only on the characteristics of the laser.

In this article, we describe recent research that we have conducted in MMW communications systems using photonicly generated carrier frequencies. We first describe the dual-wavelength laser used to generate the optical carriers and then discuss generation of the MMW carrier via photomixing of the dual-wavelength optical signals in the photodiode. We then describe the single-sideband data-encoding method and two sets of experiments conducted at 40 and 60 GHz.

PHOTONIC GENERATION OF MMW SIGNALS

There are a number of ways to produce electronic frequencies using photonic generation, including photomixing,⁶ quantum cascade lasers,⁷ and laser pulse techniques.⁸ Of these, photomixing is capable of generating continuous, stable, variable-frequency electronic signals. In photomixing, two optical signals separated in (optical) frequency by f_{RF} are combined onto a high-speed photodiode. An electrical signal at the desired RF carrier frequency (f_{RF}) is generated as the beat frequency between the optical fields. The current in the photodiode is proportional to the incident electric field through

$$i(t) = \eta E^2(t), \quad (1)$$

where η is the photodiode responsivity. When the incident electric field has components at two frequencies, the electric field can be given by

$$E(t) = A_1 \cos(2\pi f_1 t) + A_2 \cos(2\pi f_2 t + \varphi), \quad (2)$$

where A is amplitude and φ is a phase offset of the second signal. The photodiode current is then

$$i(t) = \eta \left\{ \begin{aligned} &A_1^2 + A_2^2 + A_1^2 \cos(4\pi f_1 t) + A_2^2 \cos(4\pi f_2 t + 2\varphi) \\ &+ A_1 A_2 \cos[2\pi(f_1 - f_2)t - \varphi] + A_1 A_2 \cos[2\pi(f_1 + f_2)t + \varphi] \end{aligned} \right\}. \quad (3)$$

The double frequency terms ($f_1 + f_2$, $2f_1$, $2f_2$) are at optical frequencies and can be ignored; the dc terms are not transmitted by the antenna and are likewise ignored, leaving only the MMW term of interest

$$i(t) = i_0 \cos(2\pi f_{\text{RF}} t), \quad (4)$$

where $f_{\text{RF}} = f_1 - f_2$. The responsivity and amplitudes have been folded into the peak photocurrent i_0 , and φ has been dropped because it represents an arbitrary phase offset in Eq. 4.

MMW CARRIER SIGNAL GENERATION

In our method, the two optical signals that are mixed on the photodiode are produced by a single fiber laser whose gain mechanism is SBS.⁹ This laser^{10–13} is described in detail by Gross et al. in this issue. The laser is a simple fiber ring resonator with regularly spaced resonances. The resonances have a full width at half maximum of 0.5 MHz, and the spacing of these resonances—the free spectral range of the fiber ring resonator—is 10.3 MHz. The resonator is pumped at two simultaneously resonant optical frequencies by modulating a single starting wavelength to generate a pair of sidebands that are resonant with the fiber ring resonator. Each pump produces a gain band downshifted in frequency by the Brillouin shift, which is 10.9 GHz for the selected fiber type and operating wavelength (~ 1550 nm). These

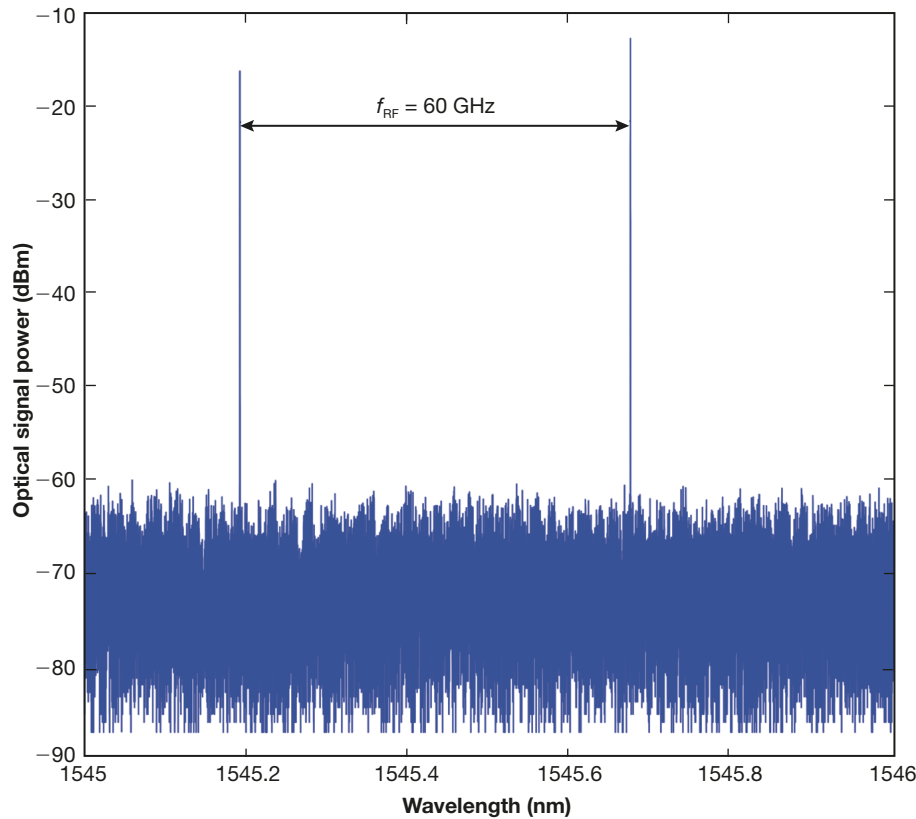


Figure 1. Measured optical spectrum of the SBS laser.

gain bands have a full width at half maximum of ~ 15 MHz, so at least one resonance will fall under each band, and each gain band yields a lasing line at whichever cavity resonance is nearest its gain peak. Because SBS is a back-scattering phenomenon, the lasing lines propagate in the direction opposite the pumps, and they must be separated from the pumps with an optical circulator. Figure 1 illustrates an exemplary laser output spectrum with the two wavelengths separated by 0.48 nm, or 60 GHz in frequency, as used in our experiments.

The beat-note frequency can be changed by tuning one or both pump frequencies, so long as both pumps remain resonant in the cavity. Thus, the beat note must be a multiple of the free spectral range. Usefully, the two pump lines can be almost arbitrarily far apart; we have demonstrated production of beat notes from 0.5 to 100 GHz, and higher frequencies are possible by using two independent pump lasers (rather than a single modulated pump laser) and a higher-bandwidth photodiode.

The properties of this laser and its Brillouin gain mechanism yield interesting and useful noise behavior.^{14, 15} First, because the two lasing lines share a common cavity, most of the environmental noise sources (e.g., thermal drift and acoustic pickup) are canceled out when the two modes are photomixed. Second, each gain band is completely independent (because each has an independent pump) and supports one and only

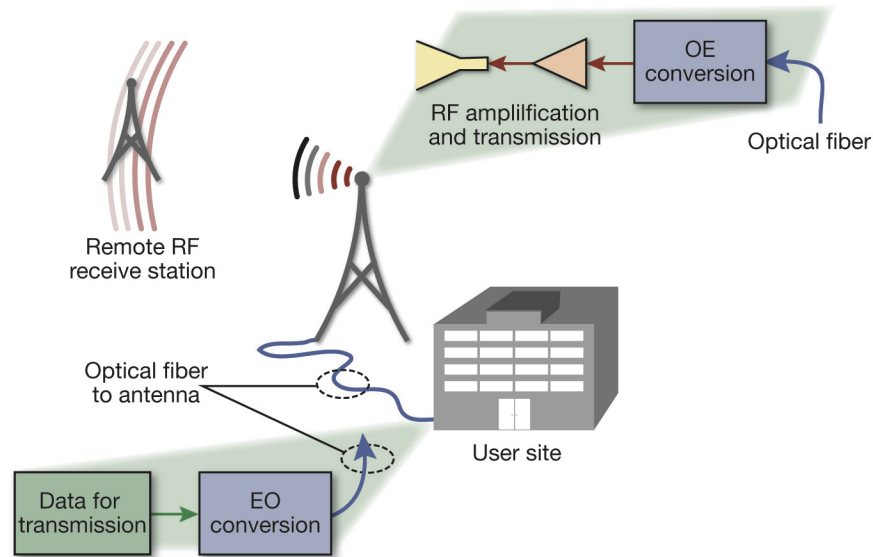


Figure 2. Fiber-wireless communications system architecture, illustrating electrical-to-optical (EO) conversion, fiber uplink to the antenna, and optical-to-electrical (OE) conversion for free-space RF transmission.

one lasing mode (this is because of a phenomenon known in the laser physics field as homogeneous broadening¹⁶). These two facts in combination eliminate competition between the two lasing wavelengths, which would otherwise generate noise in both frequency and amplitude. Finally, note that the precise lasing frequencies are determined by the positions of the resonances, rather than the gain bands, because the gain bands are ~ 30 -fold broader than the resonances. This fact strongly suppresses any transfer of noise from the pump source to the lasing lines; we have shown suppression of ~ 18 dB.¹⁷

DATA ENCODING OF PHOTONIC-TO-MMW SIGNALS

Figure 2 illustrates the overall architecture of a typical fiber-wireless communications link. Photonic communication systems consist of an EO conversion, a length of optical fiber to remote the signal, and an OE conversion. The EO conversion imposes the RF signal of interest onto an optical carrier for transport over optical fiber to a desired location, which may be kilometers away. This architecture exploits the high bandwidth and low loss capabilities of optical fiber. At the remote antenna site, an OE conversion is performed, extracting the RF information for transmission to the receiver. The RF information may be encoded onto the intensity, the phase, or the frequency of a single-wavelength optical carrier, such as the output of a laser, by using corresponding EO and OE conversion technologies.

One of the simplest methods of digital data encoding is amplitude-shift keying, which represents binary data

as two distinct signal amplitudes readily distinguished by a thresholding operation. The amplitudes may be shifted between a maximum amplitude, represented by 1, and zero amplitude, represented by 0; this shifting is referred to as on-off keying. Multiple amplitude levels may be used to represent multiple digital bit streams, thereby increasing the data throughput without increasing the signal bandwidth. Phase-shift keying is an alternative method of digital encoding that represents digital signals as two different phases of the carrier signal. The two phases are generally spaced 180° apart so that mixing with a continuous-wave signal of the same frequency will produce constructive and destructive interference,

resulting in a binary signal that can be decoded in the same manner as a simple amplitude-shift keying signal. Multiple phase levels may also be encoded, representing multiple digital bit streams.

It was noted above that the fiber span from the EO to the remote antenna may be kilometers in length. The primary limitation encountered when transporting broadband optical signals over long distances is chromatic dispersion:¹⁸ The index of refraction of silica optical fiber varies with optical frequency, which causes the different frequency components comprising the encoded signal to propagate at different velocities in the optical fiber. Standard intensity modulation of a single optical wavelength with an RF signal will generate two opti-

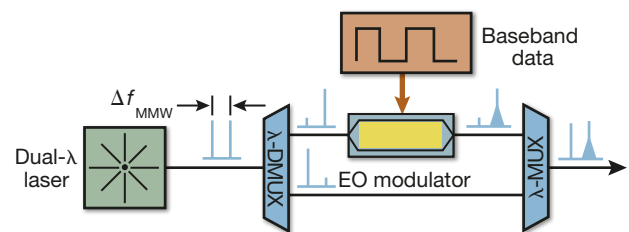


Figure 3. Diagram showing the single-sideband modulation technique. The light blue lines represent the spectral location of the optical tones at various points in the process and are separated by the desired MMW carrier frequency denoted by Δf_{MMW} . The two carriers are initially demultiplexed and one is modulated with the desired baseband data while the other is unaffected. After multiplexing, the optical signal contains modulation on one wavelength only. λ , wavelength; DMUX, demultiplexer; MUX, multiplexer.

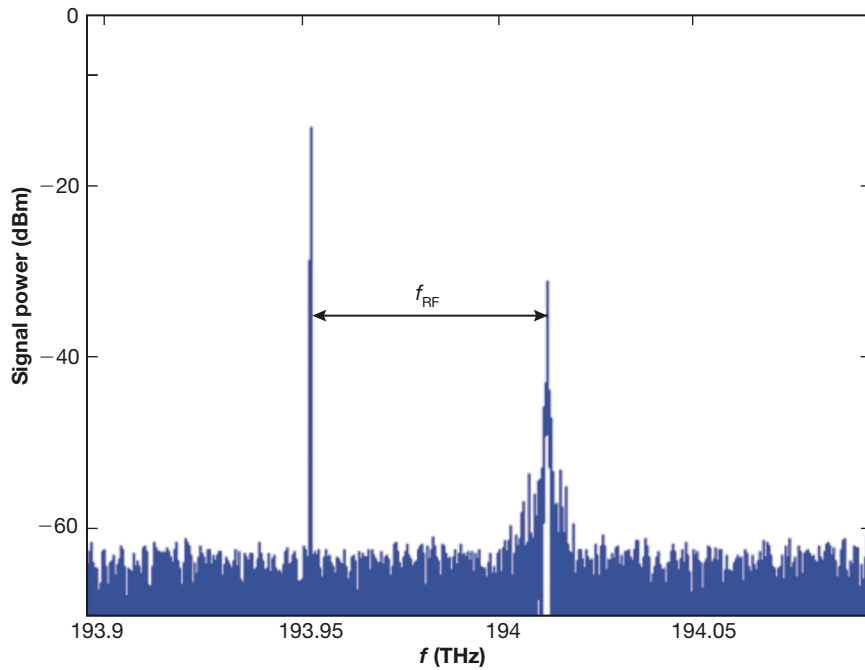


Figure 4. Measured optical spectrum with single-sideband modulation.

cal sidebands, each separated from the original source wavelength by the RF carrier frequency. Because of dispersion, the two sidebands will experience a differential time delay. Because the RF signal of interest is generated by photomixing of each sideband with the carrier, this time delay will cause periodic destructive interference between the two mixing products. In the RF domain, this manifests as periodic fading of the RF carrier as the fiber length is increased, placing limitations on the exact length of fiber that can be used for a given application. In this research, the dispersion problem is eliminated by using a dual-wavelength optical carrier and by encoding only one wavelength of the optical signal with the baseband data to be transmitted; this process is illustrated in Fig. 3. The two wavelengths output by the dual-wavelength laser are demultiplexed using an optical splitter and two optical filters. The EO modulation is then performed on one of the individual wavelengths before the optical signals are recombined. Figure 4 shows an example of the resulting optical spectrum of the recombined wavelengths; comparison with Fig. 1 shows that the higher-optical-frequency tone is carrying the encoded data. Because only one sideband is modulated, the dispersion affects only the bandwidth of the RF signal (in this example, ~ 2 GHz), rather than the bandwidth of the optical signal (i.e., the separation of the two optical wavelengths, ~ 60 GHz). The optical signal is downconverted to MMW through photomixing in the photodiode. The unmodulated optical wavelength undergoes dispersion relative to the modulated optical

signal; however, as noted in Eq. 4, the phase of the unmodulated reference signal is arbitrary and thus does not affect the generation of the MMW signal at the photodiode.

DISPERSION TOLERANCE

To demonstrate that our system is robust against dispersion-induced fading, we measured the detected power of the 60-GHz RF carrier while varying the length of fiber in the system. For comparison, we repeated the experiment for the case of a conventional photonic link, using intensity modulation of a single optical carrier to generate the 60-GHz signal. The results are shown in Fig. 5, with our system performance shown in blue. The conventional photonic link,

shown in red, experiences a null in signal power at a remoting distance of 1300 m. Shown in purple is the best fit to a raised cosine function, which characterizes the dispersive fading. As is seen from the data, the interference pattern exhibits a horizontal offset of the peak normalized power, such that the peak occurs at ~ 370 m of remoting fiber rather than zero. This is due to chirp induced by the LiNbO_3 modulator.¹⁹ By contrast

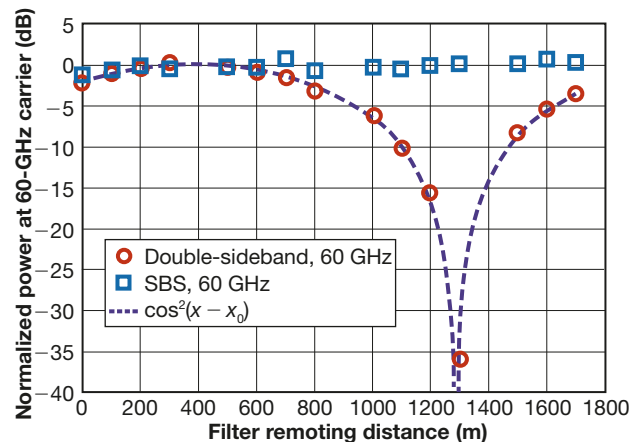


Figure 5. Received power at the 60-GHz carrier as a function of fiber length for different carrier generation methods. Circles denote the conventional method of modulating a single-optical carrier, and squares denote our dual-wavelength generation method. The dashed line is a raised cosine fit to the conventional method data.

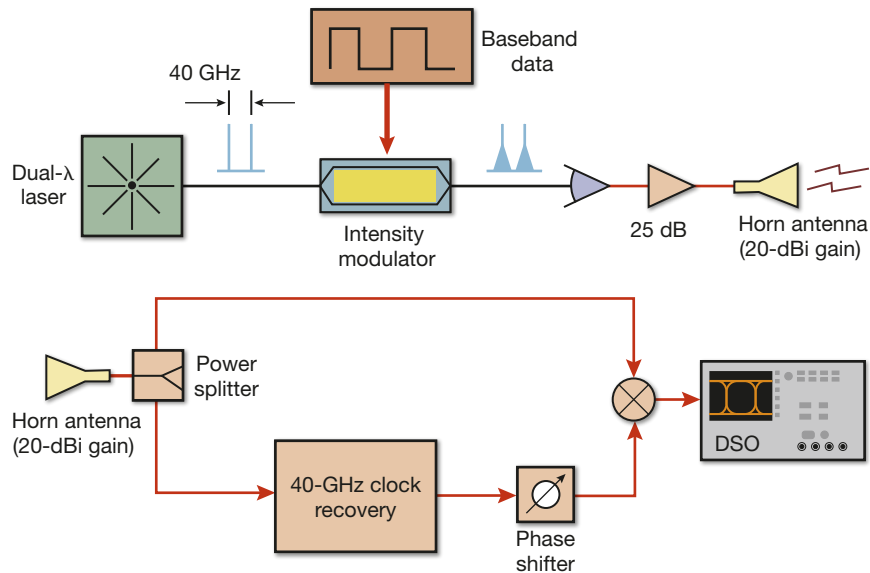


Figure 6. (Upper) System block diagram of the 40-GHz transmitter. (Lower) System block diagram of the 40-GHz receiver. DSO, digital sampling oscilloscope; λ , wavelength.

with the single-optical-carrier architecture, our SBS-generated source does not suffer from signal fading due to dispersion.

40-GHz TRANSMISSION EXPERIMENT

Our preliminary feasibility demonstrations of photonic data upconversion used the SBS laser with a wavelength separation of 40 GHz. For these experiments, the data were encoded using an intensity modulator, which encoded the baseband digital data onto both optical carriers using on-off keying at a data rate of 1 Gb/s. The architecture is shown in Fig. 6. The photodiode output was amplified with a 25-dB-gain low-noise amplifier and was transmitted over a distance of 2 m between two 20-dBi horn antennas. The received data signal was split with a power divider. One branch was input to a mixer while the other went to a clock recovery circuit which recovered the carrier tone. The recovered carrier frequency is input to the local oscillator port of the mixer and is phase adjusted to optimize downconversion of the data to baseband.

The data were analyzed on an oscilloscope; Fig. 7 shows an eye diagram of typical received baseband data. The eye diagram shows the time-domain signal superim-

posed on itself multiple times, and the “opening” is smaller when more errors are present in the data. A standard measure of the performance of a communication system is the ratio of incorrect bits received to the total number of bits in a data stream, called the bit error ratio (BER). Bit errors can be caused by a number of factors, including system noise and signal distortion. The wide opening of the eye in Fig. 7 is indicative of very low error rate; in this series of experiments, error-free ($\text{BER} < 1 \times 10^{-12}$) transmission was demonstrated over the short free-space link.

60-GHz TRANSMISSION EXPERIMENT

A primary focus of our research program has been development of photonic technologies to support WPAN applications, operating in the 54–64 GHz frequency band. Figure 8 illustrates the 60-GHz communication system we have designed using the SBS dual-wavelength laser as the MMW carrier generator, consisting of a MMW photonic transmitter and a separate MMW receiver. For this system, binary-phase-shift keying (BPSK) was used. Digital data were generated by a pulse pattern generator and modulated onto one of the demultiplexed optical sidebands using a phase modulator, encoding the binary data values onto its

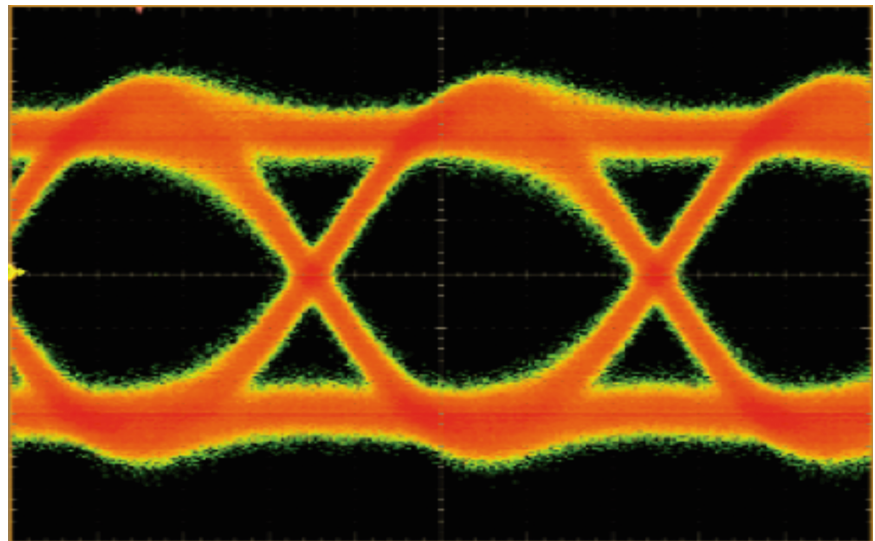


Figure 7. Eye diagram of baseband BPSK data with 1-Gb/s data rate after free-space transmission at 40 GHz over 2 m and demodulation.

optical phase. The optical signals were then combined and transported over optical fiber (distances of up to ~ 1 km in various configurations). At the photodiode, the baseband data signal is upconverted onto the 60-GHz carrier through photo-mixing—in effect, the optical phase modulation is converted to an equivalent modulation of the phase of the RF carrier. The MMW signal was amplified with a power amplifier with 22 dB of gain and transmitted to the receiver via a horn antenna with a gain of 24 dBi. The receiver consisted of an identical horn antenna, followed by a 19-dB gain low-noise amplifier. Because of the high carrier frequency, and the BPSK encoding, the receiver electronics diagram depicted in Fig. 8 is necessarily more complex than the corresponding diagram in Fig. 6. The 60-GHz signal was first downconverted to an intermediate frequency of ~ 6 GHz by mixing the received signal with a 56-GHz RF local oscillator (generated by 4-fold frequency multiplication of a 14-GHz reference oscillator). The intermediate frequency signal was then mixed with the 6-GHz output of a dielectric resonator oscillator to downconvert the data to baseband. The phase error between the intermediate frequency and the dielectric resonator oscillator is monitored with a proportional-integral-differential servo controller, the output of which is used to close the phase-locked loop on the frequency of the 14-GHz reference oscillator. The baseband data are recorded using either a telecommunications bit-error detector or a fast oscilloscope.

Initial experiments were conducted to verify system functionality and to explore bandwidth limits. The transmit-

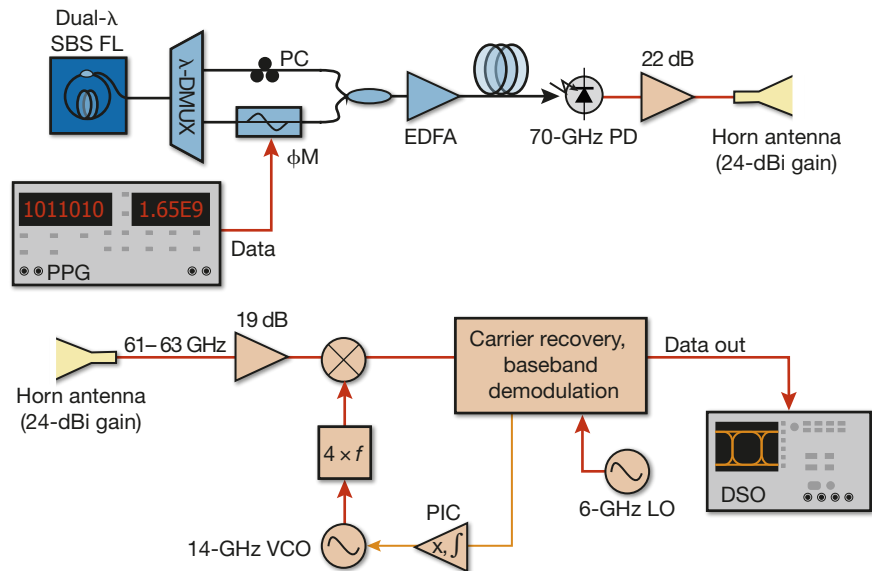


Figure 8. (Upper) System block diagram of the 60-GHz transmitter. (Lower) System block diagram of the 60-GHz receiver. λ , wavelength; ϕM , phase modulator; DMUX, demultiplexer; DSO, digital sampling oscilloscope; EDFA, erbium doped fiber amplifier; MUX, multiplexer; FL, fiber laser; LO, local oscillator; PC, polarization controller; PD, photodiode; PIC, proportional-integral controller; PPG, pulse pattern generator; VCO, voltage-controlled oscillator.

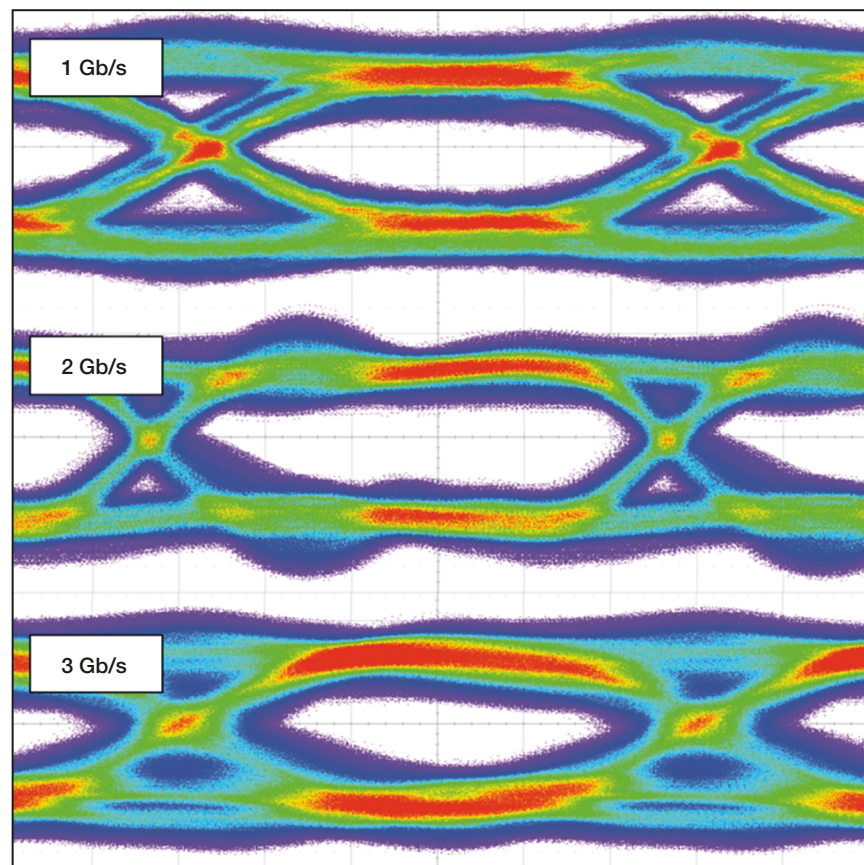


Figure 9. Eye diagrams of baseband BPSK data with data rates of 1, 2, and 3 Gb/s after free-space transmission at 60 GHz over 1.65 m and demodulation.

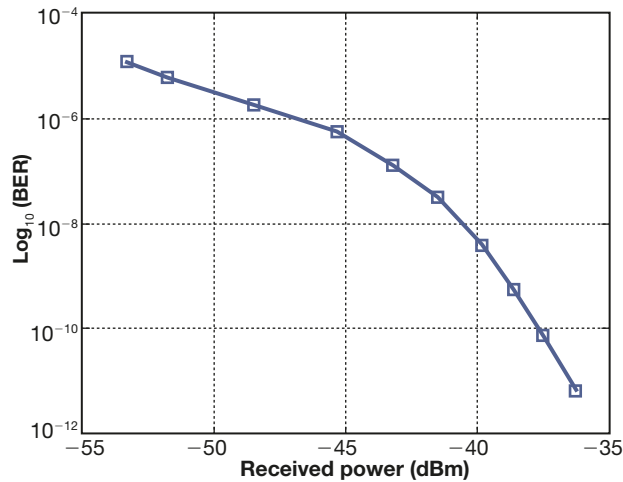


Figure 10. Measured BER for the 1.65-m link with a data rate of 1.65 Gb/s.

ter and receiver horns were placed 1.65 m apart, and the baseband data were recorded on a LeCroy oscilloscope. Figure 9 shows eye diagrams of the demodulated BSPK data with data rates of 1, 2, and 3 Gb/s. Operation at >3 Gb/s was limited by the bandwidth of the receiver hardware. The clear openings in the eye diagrams of Fig. 9 indicate low BER for each data rate. The BER was measured on the communication system as a function of received power by varying the amplification of the photodiode signal. In Fig. 10, the log of the BER is plot-

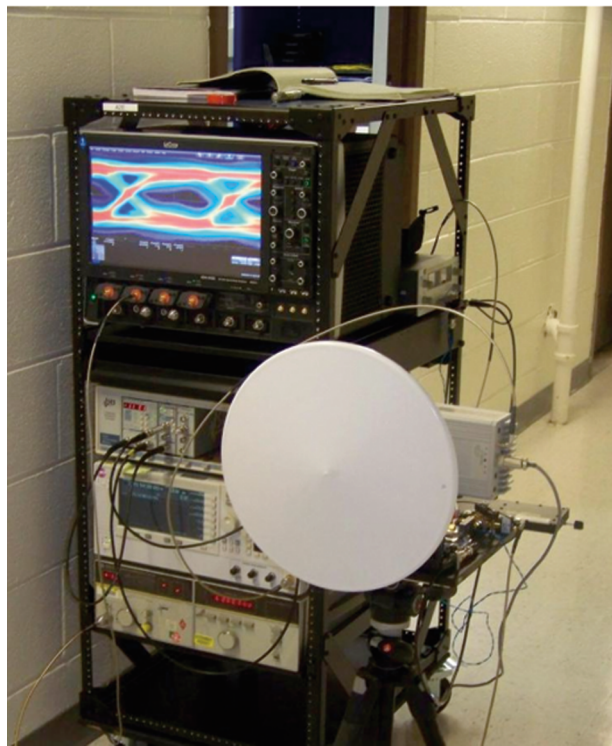


Figure 11. 60-GHz receiver setup for hallway testing.

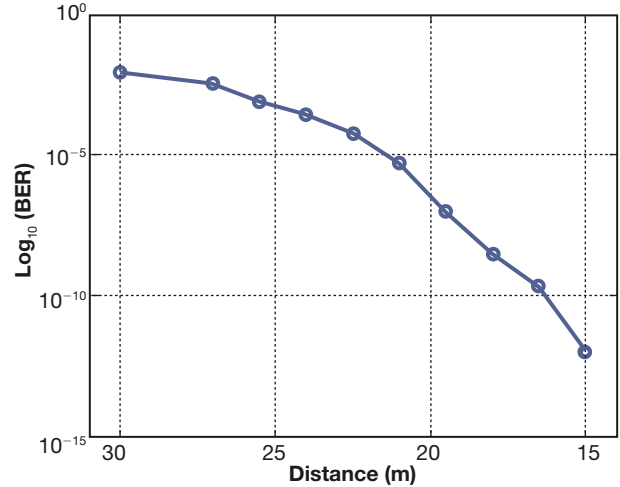


Figure 12. Measured BER for the 60-GHz hallway test with a data rate of 1.65 Gb/s.

ted against the received power. A BER of 10^{-9} or less is essentially error-free, while error-correcting codes can be reliably used with BER up to $\sim 5 \times 10^{-5}$ for common code formats (or to $>10^{-3}$ for more modern codes). At the lowest power level in this test, the BER was 4.9×10^{-5} , whereas the highest power was error-free.

To characterize the performance over longer distances, the transmitter and receiver were separated by distances up to 30 m in an indoor hallway. For these tests, the transmitter used a 16-dBi gain circular horn antenna with a beamwidth of approximately 30° , while the receiver used a 46-dBi reflector antenna with a 0.9° beamwidth. The transmitter photodiode, high-power amplifier, and antenna were mounted to a tripod, and the dual-wavelength optical signal was remoted to the photodiode from a laboratory workbench over 100 ft of optical fiber. The transmitter antenna was moved from a range of 15 m to the receiver to a range of 30 m, transmitting a constant power of approximately 0 dBm. Figure 11 shows the receiver setup with the parabolic reflector antenna. The measured BER is shown in Fig. 12, showing the expected decrease in errors as the distance decreases (note that the x axis plots the decreasing range), which results in increased received power.

ADDITIONAL APPLICATIONS AND FUTURE DIRECTIONS

The communication system in this research was developed to demonstrate photonic technologies enabling very-high-bandwidth wireless data links for moderate-length point-to-point and WPAN links operating in the 60-GHz frequency band. This frequency coincides with a strong absorption feature of atmospheric oxygen (O_2) with peak attenuation of ~ 15 dB/km,²⁰

which limits the transmission distance of signals to a few kilometers at most. Although such attenuation precludes long-distance transport, it can be used to great advantage in systems utilizing frequency reuse. Because of the limited transmission distance, the Federal Communications Commission has allocated this band (57–64 GHz, specifically) for unlicensed use,³ opening the potential commercial development of multi-gigabit-per-second cellular networks (using kilometer-scale cells) and WPANs (using room-size cells). The underlying physical layer distribution backbone for both types of networks will certainly be based on optical signal transport over optical fiber. The photonic signal generation technology developed in this research is ideally suited to such systems.

Development of commercial WPAN and broadband data networking in the 60-GHz band will impact military applications as well. The band is ideally suited for short-range secure communications because the high atmospheric absorption makes intercepting the wireless signals impossible at longer ranges. This is especially useful in situations requiring covert communications, such as special-forces operations.²¹ High-gain phased arrays at 60 GHz can be very compact because of the short wavelength and can be made thin and conformal, all of which are advantageous in a battlefield environment. These benefits could be potentially beneficial for military soldier-to-soldier communications. With regard to Navy applications, a fiber-distributed, star architecture WPAN system, such as is enabled by our work, is particularly useful in a shipboard context: Compared with copper-based physical layers, the required optical fiber backbone would require little space, is impervious to electromagnetic interference, and can support multi-gigabit-per-second data rates to numerous individual nodes (e.g., one per compartment) operating in the 60-GHz band.

Although this work has focused on 60 GHz for the reasons noted above, the basic concepts are readily transferred to other frequency bands. In particular, we have demonstrated the capability of photonicly generating RF frequencies up to 100 GHz. Higher-frequency MMW bands have been allocated by the Federal Communications Commission (at 71–76, 81–86, and 92–95 GHz) for potential development for broadband wireless networking.³ Compared with 60 GHz, atmospheric attenuation at these higher frequencies is greatly reduced (as low as ~0.2 dB/km at sea level, depending on weather conditions), which makes it possible to greatly expand the reach of a MMW link. Potential military applications are numerous, including high-bandwidth ship-to-ship communications, downlinking of data from unmanned aerial vehicles, and very-high-bandwidth satellite communications. We are actively pursuing extension of the technologies discussed in this article into this regime.

ACKNOWLEDGMENTS: We gratefully acknowledge the cooperation and input of Dalma Novak and Rodney Waterhouse of Pharad, LLC during the course of this research. This work was funded by the National Science Foundation under joint Small Business Technology Transfer Grant IIP-0924028 with Pharad, LLC of Glen Burnie, Maryland.

REFERENCES

- ¹Currie, N. C., and Brown, C. E., *Principles and Applications of Millimeter-Wave Radar*, Artech House, Norwood, MA (1987).
- ²Taylor, G. B., Carilli, C. L., and Perley, R. A. (eds.), *Synthesis Imaging in Radio Astronomy II*, Astronomical Society of the Pacific, San Francisco (1999).
- ³Wells, J., "Faster Than Fiber: The Future of Multi-Gb/s Wireless," *IEEE Microwave Magazine* **10**(3), 104–112 (2009).
- ⁴Bjarnason, J. E., Chan, T. L. J., Lee, A. W. M., Celis, M. A., and Brown, E. R., "Millimeter-Wave, Terahertz, and Mid-infrared Transmission Through Common Clothing," *Appl. Phys. Lett.* **85**(4), 519–521 (2004).
- ⁵IEEE 802 LAN/MAN Committee, *IEEE Standard for Information Technology—Telecommunications and Information Exchange Between Systems—Local and Metropolitan Area Networks—Specific Requirements. Part 15.3: Wireless Medium Access Control (MAC) and Physical Layer (PHY) Specifications for High Rate Wireless Personal Area Networks (WPANs) Amendment 2: Millimeter-wave-based Alternative Physical Layer Extension*, IEEE Standard 802.15.3c, IEEE Inc., New York (2009).
- ⁶Juggard, P. G., Ellison, B. N., Shen, P., Gomes, J. J., Davies, P. A., Shullue, W. P., Vaccari, A., and Payne, J. M., "Efficient Generation of Guided Millimeter-Wave Power by Photomixing," *IEEE Photon. Technol. Lett.* **14**(2), 197–199 (2002).
- ⁷Williams, B. S., "Terahertz Quantum Cascade Lasers," *Nat. Photonics* **1**(9), 517–519 (2007).
- ⁸Tonouchi, M., "Cutting-Edge Terahertz Technology," *Nat. Photonics* **1**(2), 97–105 (2007).
- ⁹Geng, J., Staines, S., Wang, Z., Zong, J., Blake, M., and Jiang, S., "Highly Stable Low-Noise Brillouin Fiber Laser with Ultranarrow Spectral Linewidth," *IEEE Photon. Technol. Lett.* **18**(17), 1813–1815 (2006).
- ¹⁰Dennis, M. L., Sova, R. M., and Clark, T. R., "Dual-Wavelength Brillouin Fiber Laser for Microwave Frequency Generation," in *Proc. Optical Fiber Communications Conf.*, Anaheim, CA, paper OWJ6 (2007).
- ¹¹Dennis, M. L., Sova, R. M., and Clark, T. R., "Microwave Frequency Generation up to 27.5 GHz Using a Dual-Wavelength Brillouin Fiber Laser," in *Proc. IEEE/LEOS Summer Topical Meeting*, pp. 194–195 (2007).
- ¹²Gross, M. C., Callahan, P. T., Clark, T. R., Novak, D., Waterhouse, R. B., and Dennis, M. L., "Tunable Millimeter-Wave Frequency Synthesis up to 100 GHz by Dual-Wavelength Brillouin Fiber Laser," *Opt. Express* **18**(13), 13321–13330 (2010).
- ¹³Dennis, M. L., Callahan, P. T., and Gross, M. C., "Suppression of Relative Intensity Noise in a Brillouin Fiber Laser by Operation Above Second-Order Threshold," in *Proc. 2010 23rd Annual Meeting of the IEEE Photonics Society*, pp. 28–29 (2010).
- ¹⁴Callahan, P. T., Gross, M. C., and Dennis, M. L., "Phase Noise Measurements of a Dual-Wavelength Brillouin Fiber Laser," *Proc. 2010 IEEE Topical Meeting on Microwave Photonics*, pp. 155–159 (2010).
- ¹⁵Callahan, P. T., Gross, M. C., and Dennis, M. L., "Frequency-Independent Phase Noise in a Dual-Wavelength Brillouin Fiber Laser," *IEEE J. Quantum Electron.* **47**(8), 1142–1150 (2011).
- ¹⁶Siegman, A. E., *Lasers*, University Science Books, Mill Valley, CA, pp. 126–134 (1986).
- ¹⁷Gross, M. C., Clark, T. R., and Dennis, M. L., "Narrow-Linewidth Microwave Frequency Generation by Dual-Wavelength Brillouin Fiber Laser," in *Proc. 21st Annual Meeting of the IEEE Lasers and Electro-Optics Society*, 2008, pp. 151–152 (2008).

¹⁸Lim, C., Ampalavanapillai, N., Masduzzaman, B., Lee, K.-L., Novak, D., and Waterhouse, R., "Mitigation Strategy for Transmission Impairments in Millimeter-Wave Radio Over Fiber Networks," *J. Opt. Netw.* **8**(2), 201–214 (2009).

¹⁹Wooten, E. L., Kissa, K. M., Yi-Yan, A., Murphy, E. J., Lafaw, D. A., et al., "A Review of Lithium Niobate Modulators for Fiber-Optic Communications Systems," *IEEE J. Sel. Topics Quantum Electron.* **6**(1), 69–82 (2000).

²⁰Marcus, M., and Pattan, B., "Millimeter Wave Propagation: Spectrum Management Implications," *IEEE Microwave Magazine* **6**(2), 54–62 (2005). [Reprinted from FCC Office of Engineering and Technology New Technology Development Division, Bulletin #70.]

²¹Cotton, S. L., Scanlon, W. G., and Madahar, B. K., "Millimeter-Wave Soldier-to-Soldier Communications for Covert Battlefield Operations," *IEEE Communications Magazine* **47**(10), 72–81 (2009).

The Authors



Jeffrey A. Nanzer



Patrick T. Callahan



Michael L. Dennis



Thomas R. Clark Jr.

Jeffrey A. Nanzer is a member of the Senior Professional Staff in APL's Air and Missile Defense Department. Dr. Nanzer provided expertise in MMW systems and technology, developed experiments, and conducted laboratory and field experiments. **Patrick T. Callahan** was previously a member of the Associate Professional Staff in the Electro-Optical and Infrared Systems and Technology Group in APL's Air and Missile Defense Department and is now with the Department of Electrical Engineering and Computer Science at the Massachusetts Institute of Technology. Mr. Callahan constructed and evaluated the communication system, assembled and verified subsystems, and conducted laboratory and field experiments. **Michael L. Dennis** is a Principal Professional Staff member in the Air and Missile Defense Department and the Principal Investigator on this project. Dr. Dennis provided expertise in communications, optical components, and lasers and originally developed the dual-wavelength technology used in this project. **Thomas R. Clark Jr.** is a Principal Professional Staff member in the Air and Missile Defense Department. Dr. Clark provided expertise in communications, photonics, and future applications for this research. For further information on the work reported here, contact Jeffrey Nanzer. His e-mail address is jeffrey.nanzer@jhuapl.edu.